Coarse-to-Fine Approach for Tree Point Cloud Registration Based on Relaxation Labeling

Matheus Ferreira da Silva [1], Renato César dos Santos [1,2], and Mauricio Galo [1,2]

[1] Graduate Program in Cartographic Sciences, Faculty of Science and Technology, São Paulo State University (UNESP), Presidente Prudente, São Paulo, Brazil - matheus-ferreira.silva@unesp.br
[2] Department of Cartography, Faculty of Science and Technology, São Paulo State University (UNESP), Presidente Prudente, São Paulo, Brazil - {renato.cesar, mauricio.galo}@unesp.br

Keywords: 3D Mapping, Terrestrial LASER Scanning, Feature Matching, Urban Forests, Iterative Closest Point

Abstract

Recent advances in photogrammetry and remote sensing have highlighted the advantages of three-dimensional (3D) point cloud data for accurately reconstructing different scenarios and environments, including forest and agricultural sites. Currently, LiDAR (Light Detection and Ranging) systems are widely used to acquire 3D data, offering high geometric precision and adaptability across various platforms. In comparison with conventional field surveys, information obtained by LiDAR systems provides greater spatial coverage and efficiency, particularly in large-scale applications. However, the automatic registration of point clouds in complex and irregular environments, such as forests, remains a challenge due to occlusions, repetitive patterns, and low overlap between scans. This paper proposes a coarse-to-fine point cloud registration approach designed for tree-dense environments. The method begins by processing each point cloud, acquired from different stations, to generate a Canopy Height Model (CHM). To determine tree center positions (x_c, y_c), the point clouds are sliced at breast height (1.30 ± 0.01 m), and the points corresponding to each tree cross-section are used to compute the center. These center features are subsequently matched using the relaxation labeling (RL) algorithm, which is based on probabilistic similarity and spatial relationships. From these corresponding trunk center pairs, it is possible to estimate an initial 2D transformation between the scans. This initial alignment is then refined using the Iterative Closest Point (ICP) algorithm to compute the final 3D transformation. Experiments using pairwise terrestrial scans with low overlap (< 30%) achieved a root mean square error (RMSE) of approximately 3 cm, without the use of artificial registration targets.

1. Introduction

Light Amplification by Stimulated Emission of Radiation (LASER) enables the acquisition of three-dimensional data with high geometric accuracy by emitting and digitizing light beams reflected by the surface of objects. LiDAR (Light Detection and Ranging) is one of the most prominent technologies in the field of mapping domain (Vosselman and Mass, 2010; Shan and Toth, 2018; Luhmann et al., 2020), and it has been applied in industrial and close-range surveying, construction, urban planning, architectural inspection, forest monitoring (Shao et al., 2020), and agricultural management (Jin et al., 2021).

In the context of natural resources and precision agriculture, LiDAR-derived data have been utilized for plant phenotyping (Roitsch et al., 2019; Chebrolu et al., 2021; Da Silva et al., 2025), yield estimation (Méndez et al., 2019), and optimized fertilizer and pesticide application (Wu et al., 2020), among other applications. Scientific studies in this area address data acquisition strategies, sensor calibration, information extraction, multisensor data integration, and point cloud registration (Riveiro and Lindenbergh, 2019).

Mapping a scene or object with LiDAR generally requires multiple scans from different viewpoints to cover all surfaces. To generate a complete model, these scans must be co-registered into a unified coordinate system through 3D coordinate transformations. According to Wolf, Dewitt, and Wilkinson (2014), scan registration can be achieved in three main ways: (1) using common reference targets between scans, (2) employing GNSS (Global Navigation Satellite System) and INS (Inertial Navigation System) data from onboard sensors, or (3) matching scan points.

Target-based registration can be a laborious and time-consuming task (Jin et al., 2021), as target positions must be precisely identified and carefully placed to appear in almost all scans (Liang et al., 2012). Although GNSS and INS provide accurate positioning and orientation, they are subject to limitations such as signal loss, electromagnetic interference, INS drift, and multipath effects. These issues are particularly problematic in forested or agricultural environments, where obstructions and signal degradation are common.

Matching-based registration approaches rely on the scan data, either directly through point clouds or via extracted geometric primitives (real or virtual), to estimate transformation parameters (Vosselman and Mass, 2010). Standard methods include the Iterative Closest Point (ICP) algorithm (Besl and McKay, 1992) and the Normal Distribution Transform (NDT) proposed by Biber and Strasser (2003) and modified by Magnusson, Lilienthal, and Duckett (2007).

Although various approaches have been proposed for registering point clouds, existing methods are suitable for scenarios with slight variation in point cloud density and homogeneous overlap between scans, as in indoor and urban environments (Shao et al., 2020). Therefore, registering point clouds captured in agricultural and forestry scenarios can be a challenge, as it involves scenes with repetitive patterns, making matching difficult due to ambiguity, occlusions, and low overlap between point clouds.

To address some of these challenges, this paper makes the following contributions:

- Proposal of an automatic coarse-to-fine point cloud registration approach that uses only features extracted from tree trunks, eliminating the need for artificial targets or auxiliary sensor data.
- Propose the use of relaxation labeling (RL) concept to match geometric features in environments characterized

This contribution has been peer-reviewed. The double-blind peer-review was conducted on the basis of the full paper.
https://doi.org/10.5194/isprs-annals-X-3-W4-2025-93-2026 | © Author(s) 2026. CC BY 4.0 License.

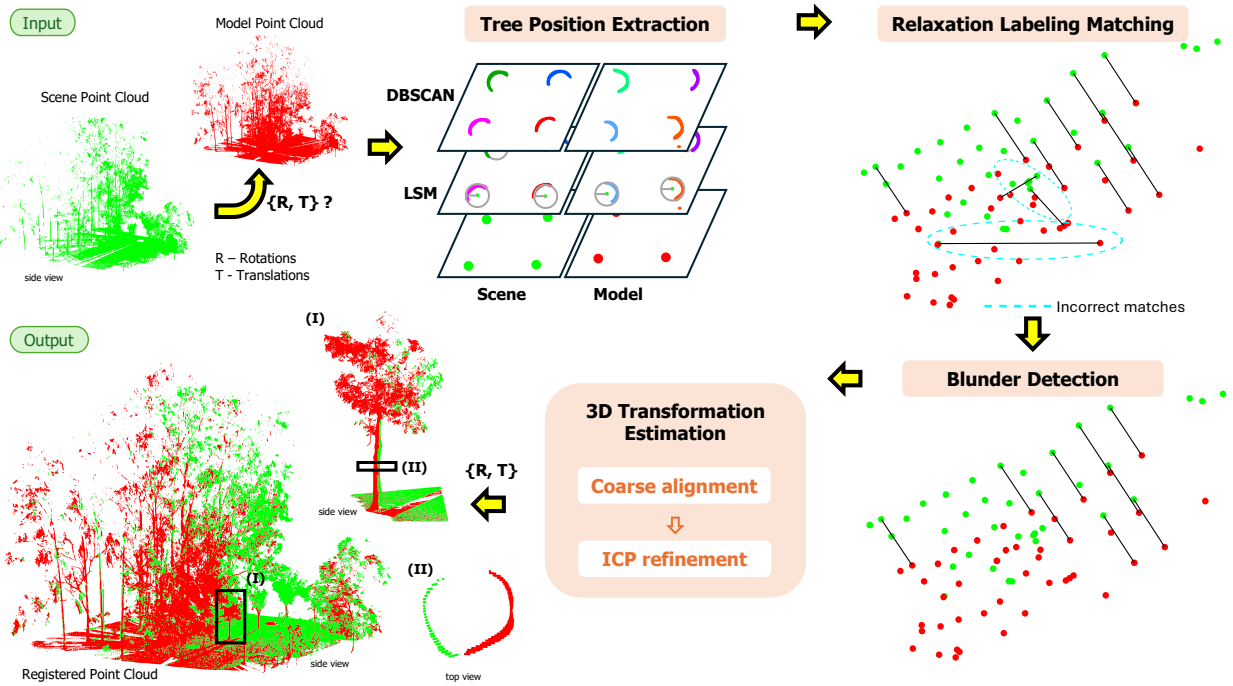

Figure 1. Flowchart of the proposed point cloud registration approach based on relaxation labeling.

by high ambiguity and low overlap, such as urban forest trees, a context in which, to the best of our knowledge, it has not previously been applied.

2. Related Works

Point cloud registration is an essential process for mapping objects and environments using LiDAR sensors and photogrammetric reconstruction techniques. Over the years, various methods for point cloud registration have been proposed. Early approaches relied primarily on point correspondences, such as the ICP algorithm, while subsequent methods incorporated geometric primitives and probabilistic models, including the NDT. More recently, deep-learning-based techniques have emerged, designed to extract and use robust features directly from raw point clouds.

Several studies have proposed taxonomies for registration techniques in this context. Xu et al. (2024), for instance, classify registration methods into two main categories: feature-based registration and error minimization. Feature-based methods extract and match geometric descriptors such as key points, edges, surfaces, and curvature patterns. In contrast, error minimization methods aim to optimize transformation parameters by minimizing distance metrics or aligning probabilistic distributions between sets of points.

In practice, registration methods often combine elements from multiple categories to address challenges related to the environment, acquisition platform, or sensor characteristics. This diversity has given rise to a wide range of techniques, as well as numerous review papers that synthesize advances and highlight persistent challenges in this field. Historically, most studies focused on adaptations of ICP-based approaches.

The ICP algorithm (Besl and McKay, 1992) is still one of the most widely adopted techniques for precise registration. It identifies corresponding point pairs within overlapping regions using the shortest Euclidean distance. These pairs are then used to compute the six parameters of a rigid-body transformation (three translations and three rotations). Nevertheless, ICP requires sufficient overlap and a good initial alignment, making it most effective in structured environments, such as indoor or urban scenes, whereas its applicability in natural settings remains limited.

More recently, attention has turned to deep learning-based methods. These approaches aim to leverage the capacity of neural networks to learn feature representations and transformations directly from data. A study by Monji-Azad et al. (2023) demonstrated that learning-based methods can handle non-rigid transformations, particularly when point cloud deformation occurs due to object motion or sensor variability. Although progress has been made, deep learning techniques still rely on annotated datasets, require lengthy training processes, and face challenges in adapting to different environments.

3. Point Cloud Registration Approach

3.1 Tree Position Extraction

A general overview of the proposed point cloud registration approach is depicted in Figure 1, with each step described sequentially. Prior to tree position extraction, the point cloud was normalized using the adaptive Cloth Simulation Filtering (CSF) algorithm (Lin et al., 2021). This algorithm extends the original cloth simulation approach (Zhang et al., 2016), enabling the generation of a Digital Terrain Model (DTM) even in areas with sparse ground point distribution. The normalization process yields a height-normalized point cloud, in which the point's elevation is expressed relative to the local ground surface. Ground points are assigned a value of 0 m, while object points (e.g., trees) are assigned their vertical distance above the ground. This stage produces the Canopy Height Model (CHM). A horizontal slice of the point cloud at breast height (1.30 m ± 0.01 m) was then extracted for each scanning station to estimate the tree's position, since this reference height is widely adopted for dendrometric measurements.

This contribution has been peer-reviewed. The double-blind peer-review was conducted on the basis of the full paper.
https://doi.org/10.5194/isprs-annals-X-3-W4-2025-93-2026 | © Author(s) 2026. CC BY 4.0 License.

Points within the breast height slice were grouped using the Density-Based Spatial Clustering of Applications with Noise (DBSCAN) algorithm (Ester et al., 1996). DBSCAN identifies dense clusters while filtering out noise in sparse regions, requiring two parameters: neighborhood radius (ε) and minimum cluster size (min_{Pts}). For each cluster, a circular cross-section was fitted using General Least Squares Adjustment (Mikhail, 1976) to estimate tree trunk radius (r) and the center coordinates of each slice (x_c, y_c), which were subsequently used to determine tree locations.

3.2 Relaxation Labeling-Based Candidate Matching

The estimated positions of the tree centers were used as candidate features for pairwise registration between scanning stations (Model - M and Scene - S). Initial matching was performed using an RL algorithm in the 2D plane (XY). Similarity values for all candidate matches were initially set with equal weight ($p_{ij} = 1$), assuming no prior feature-based correspondences.

Compatibility between candidate matches was computed based on the spatial distribution of each point and its K-nearest neighbors (K_n), following the approach proposed by Zhang et al. (1994). This involves calculating the Euclidean distance between a pair of objects i and i_k in the M set, and j and j_k in the S set. The mean distance is given by Equation 1, which is used to calculate the relative distance measure (r_{dm}) (Equation 2). If the distance between corresponding object pairs is preserved, the value of r_{dm} is zero.

$$dist(i,j;i_k,j_k) = \frac{d(i,i_k) + d(j,j_k)}{2} \tag{1}$$

$$r_{dm} = \frac{|d(i,i_k) - d(j,j_k)|}{dist(i,j;i_k,j_k)} \tag{2}$$

Equation 3 defines the distance-based compatibility function. This formulation considers the K_n-nearest neighbors and the assumption that extracted features are subject to random errors. Notably, the influence of neighbors decreases with distance, emphasizing local structural similarity. The numerator of this equation includes the r_{dm} term and a relative error threshold (R_e), which can be set according to the expected LiDAR accuracy to mitigate the impact of outliers.

$$c_{ij}^{dist} = \sum_{k=1}^{Kn} \frac{\delta(i,j,i_k,j_k)}{1 + dist(i,j,i_k,j_k)} \tag{3}$$

where:

$$(i,j,i_k,j_k) = \begin{cases} e^{-\frac{r_{dm}}{R_e}}, if\ r_{dm} < R_e \\ \_ \\ 0, otherwise \end{cases} \tag{4}$$

The similarity and compatibility values are combined to update match probabilities (p_{ij}^0), where p_{ij}^0 corresponds to the initial similarity values, through an iterative stochastic process. Furthermore, the commutativity property of RL can be exploited to identify reliable correspondences. Since the solution is asymmetric—i.e., if the order of the object sets is changed, $p_{ij}(M, S)$ and $p'_{ji}(S, M)$ will differ. In this context, their intersection can be used to eliminate false matches (Galo and Tozzi, 2004).

3.3 Blunder Detection via Residual Analysis

Recognizing that feature matching constitutes an ill-posed problem (Heipke, 1996), a filtering step was implemented to remove eventual false correspondences (blunders). This step analyzes the residual vector derived from the parameters of an estimated orthogonal 2D transformation (comprising one rotation and two translations) between the candidate-matched point features. The detection process is iterative and follows these steps:

Step 1. Set $k = 0$.

Step 2. At iteration k, estimate the 2D transformation using all current matches (resulting from Section 3.2).

Step 3. Compute residuals for each match trunk ($v_{ij} \in V$) and the standard deviation of the residuals (σ_{res}^k).

Step 4. Remove the match trunk with the largest residual magnitude $|v_{ij}|$, outside the tolerance interval ($Tolerance_{min} \leq |v_{ij}| \leq 3 \times \sigma_{res}^k$), where $Tolerance_{min}$ is a threshold to prevent eliminating all correspondences.

Step 5. Update k ($k \leftarrow k + 1$) and return to Step 2. Iteration terminates when $|\sigma_{res}^{(k+1)} - \sigma_{res}^{(k)}| < 10^{-5}$, indicating convergence.

3.4 Transformation Refinement Using ICP

The transformation was initially estimated in the horizontal plane, using a coarse algorithm restricted to the XY axis. To achieve preliminary vertical alignment, the median difference in Z-coordinates between the two-point clouds (after 2D registration) was calculated and applied as an initial translation to the Scene cloud (S).

Once this coarse alignment was established, the complete 3D transformation was refined using the Iterative Closest Point (ICP) algorithm, adopting the point-to-point variant as implemented in *CloudCompare* (version 2.13.2). ICP was initialized with the combined transformation derived from the 2D parameters and the median Z difference. The algorithm then iteratively minimizes the sum of squared distances between the correspondences of nearest neighbors, updating the estimates for rotations and translations in all three dimensions (XYZ).

4. Experimental Design and Quality Assessment

4.1 Terrestrial LiDAR System

The data used in the experiments were acquired using a FARO Focus Premium terrestrial laser scanner. This LiDAR system can scan objects at distances of up to 350 m, with an accuracy of ± 1 mm for ranges between 10 and 25 m, assuming a white surface with 90% reflectivity. It operates in the near-infrared wavelength (λ = 1553.5 nm), emitting a laser beam with a divergence of 0.3 mrad. The scanner provides a 360° horizontal field of view and a 300° vertical field of view, with an angular resolution of 19 arcseconds.

4.2 Study area and data collection

The experiments were conducted in an urban forest at São Paulo State University (UNESP), Presidente Prudente, situated in the western region of São Paulo State, Brazil (22°07'21.06" S, 51°23'17.71" W). Data acquisition was carried out according to

the manufacturer's guidelines (FARO Technologies, Inc., USA) for outdoor environments under sunny conditions.

Spherical targets were placed throughout the area to enable manual registration for each scan, serving as ground-truth references to assess the performance of the proposed point cloud registration method. A total of eight scanning stations were positioned across the study site (Figure 2). The complete acquisition process took approximately one hour. For the experiments reported in this work, the pair of stations 5 (Model) and 6 (Scene) was selected.

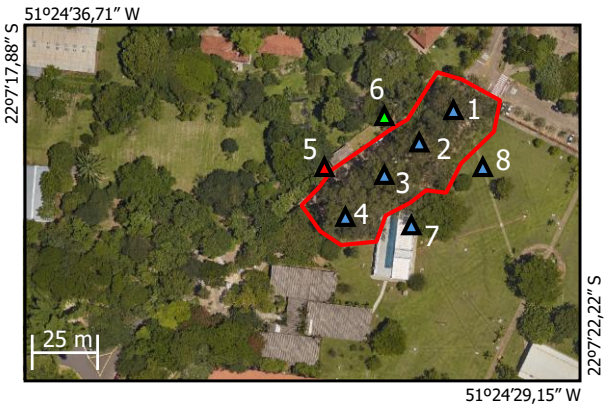

Figure 2. Spatial distribution of the eight scanning stations. The red triangle represents the Model station (scan 5), while the green triangle represents the Scene station (scan 6).

4.3 Quality Assessment

The quality of registration was evaluated using both qualitative and quantitative criteria. The qualitative assessment was based on visual inspection of the point clouds, particularly using cross-sectional views, to verify the consistency of alignment between different scans. For the quantitative assessment, the absolute discrepancies between fitted sphere centers in the Model and Scene scans were calculated. The Root Mean Square Error (RMSE) was used to measure the overall accuracy of the point cloud registration.

5. Results

Table 1 summarizes the tree center matching statistics between the Model and Scene point clouds. These results were obtained using the following parameters, established based on empirical tests: relaxation labeling (R_e = 0.02 m, K_n = 3, $p_{ij} \geq 0.90$), blunder detection ($Tolerance_{min}$ = 0.10 m), and ICP refinement (final overlap = 30%, convergence threshold = 10^{-5}).

Description	Number
Extracted tree centers (M)	44
Extracted tree centers (S)	36
All possible matches between the M and S sets	27
Matches identified by the RL algorithm	12
Incorrect matches removed from blunder detection	3
Final matches	9

Table 1. Summary of extracted tree centers, matching results, and blunder detection statistics.

Figure 3 illustrates the matches (a), counter-matches (b), and the intersection solution (c) obtained from the RL algorithm. Only correspondences with a similarity score greater than 0.90 are shown. Incorrect matches are highlighted with dotted ellipses in Figure 3(c) for visual identification.

Based on the evaluation of four sphere targets distributed in the overlap area, the RMSE values for the discrepancies in sphere center positions were $RMSE_X$ = 2.71 cm, $RMSE_Y$ = 1.98 cm, $RMSE_Z$ = 0.52 cm, and $RMSE_{XYZ}$ = 3.39 cm for the resultant. Figure 4 presents a qualitative assessment of registration accuracy through visual inspection of cross-sectional views of tree trunks, allowing evaluation of local alignment consistency between the point clouds.

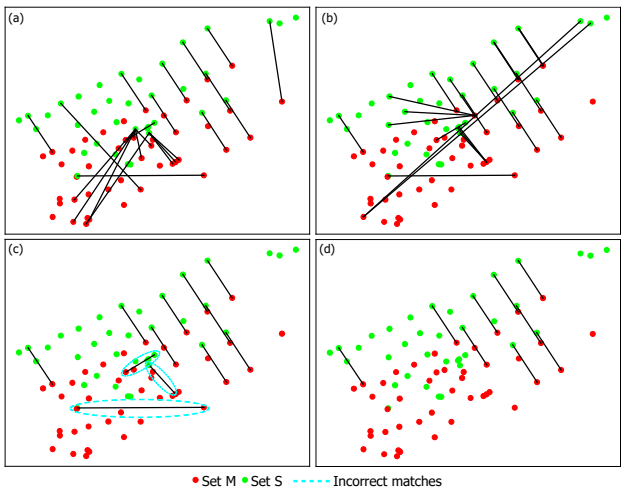

Figure 3. Results of the relaxation labeling algorithm applied to the Model and Scene sets. (a) Correspondence solution p_{ij}(M, S), (b) Counter-correspondence solution p_{ji}'(S, M), (c) Intersection of both solutions, and (d) Final matches after blunder matches removal.

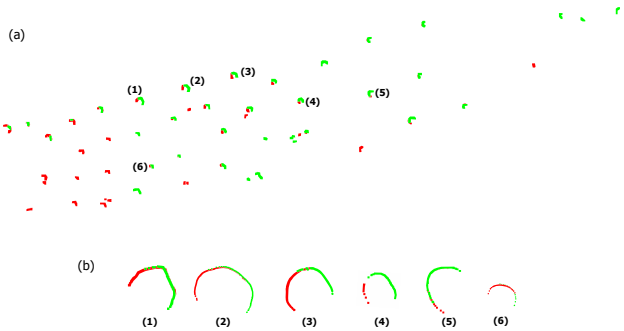

Figure 4. Visual result of point cloud registration applied to cross-sections at breast height for a pair of clouds (M, S) used in the experiments (a), and details of the arrangement of the points of the two clouds, for six trunks (b).

6. Discussion

The proposed approach was evaluated on a pair of point clouds of an urban forest with less than 30% overlap, using the tree position as a feature to match point clouds. The quantitative indicator based on sphere targets resulted in an $RMSE_{XYZ}$ of approximately 3 cm, without the use of artificial targets.

The relatively low error in the vertical component ($RMSE_Z$ = 0.52 cm) can be attributed to the flat terrain of the urban environment, as well as to the leveling procedure applied to the equipment during data collection. This procedure ensured that the coarse transformation could be split into sequential stages, allowing translations and rotations to be estimated in the

XY plane and the translation along the Z-axis to be estimated separately.

Considering the matching process with relaxation labeling, 12 matches were identified out of 27 possible, with 3 being incorrect and subsequently eliminated through the blunder detection approach described in Section 3.3. As presented in Table 1, out of 58 trees in the study area, 44 tree centers were identified in the Model set and 36 in the Scene set. Among these, 17 appeared exclusively in the Model (i.e., not visible in the Scene scan), while 9 appeared only in the Scene (i.e., not visible in the Model scan). These numbers highlight the impact of occlusion in terrestrial laser scanning, as many trunks become hidden depending on the scanner's position. Nevertheless, despite these challenges, the RL algorithm successfully established reliable correspondences, demonstrating robustness to partial visibility.

7. Conclusions

This paper presented an automated method for pairwise point cloud registration of tree trunks in forest and urban environments. Traditional algorithms often struggle in such scenarios due to low overlap between scans and high object similarity. The proposed coarse-to-fine approach employs relaxation labeling to establish correspondences between tree trunk centers, using relative distances as a compatibility measure. Once this initial alignment is achieved, the transformation is refined through the classical ICP algorithm. For future work, we recommend evaluating the method on larger and more diverse datasets. Possible enhancements include incorporating additional metrics into the relaxation labeling process, such as Diameter at Breast Height (DBH) and angular relations between neighbouring trunk trees.

Acknowledgments

The authors are grateful for the support provided by the Coordenação de Aperfeiçoamento de Pessoal de Nível Superior - Brazil (CAPES) - Finance Code 001; São Paulo State Research Foundation (FAPESP), Brazil (Process Numbers 2021/06029-7, 2023/14756-1, and 2025/05405-6); and National Council for Scientific and Technological Development (CNPq) (Grant n. 309734/2022-3).

References

Besl, P. J., McKay, N. D., 1992: A method for registration of 3-D shapes. *IEEE Trans. Pattern Anal. Mach. Intell.*, *14*(2), 239–256. doi.org/10.1109/34.121791.

Biber, P., Strasser, W., 2003: The normal distributions transform: A new approach to laser scan matching. *Proc. IEEE/RSJ Int. Conf. Intelligent Robots and Systems (IROS 2003), 3*, 2743–2748. doi.org/10.1109/IROS.2003.1249285.

Chebrolu, N., Magistri, F., Läbe, T., Stachniss, C., 2021: Registration of spatio-temporal point clouds of plants for phenotyping. *PLoS ONE*, *16*(2), 1–25. doi.org/10.1371/journal.pone.0247243.

Da Silva, M. F., Dos Santos, R. C., Tommaselli, A. M. G., Galo, M. 2025: Diameter at Breast Height (DBH) Estimation and Stem Cross-Section Shape Analysis of Eucalyptus Trees Using LiDAR Data after Noisy Removal. *Rev. Bras. Cartogr.*, *77*(0a). doi.org/10.14393/rbcv77n-72970.

Ester, M., Kriegel, H.-P., Sander, J., Xu, X. 1996: A density-based algorithm for discovering clusters in large spatial databases with noise. *Proc. 2nd Int. Conf. Knowledge Discovery and Data Mining*, 226–231.

Galo, M., Tozzi, C. L., 2004: Feature-point based matching: A sequential approach based on relaxation labelling and relative orientation. *J. WSCG*, *12*(1), 8. doi.org/10.13140/2.1.4175.1045.

Heipke, C. 1996: Overview of image matching techniques. *Proc. OEEPE Workshop on the application of digital photogrammetric Workstations*.

Jin, S., Sun, X., Wu, F., Su, Y., Li, Y., Song, S., Xu, K., Ma, Q., Frederic, B., Jiang, D., Ding, Y., Guo, Q., 2021: LiDAR sheds new light on plant phenomics for plant breeding and management: Recent advances and future prospects. *ISPRS J. Photogramm. Remote Sens.*, *171*, 202–223. doi.org/10.1016/j.isprsjprs.2020.11.006.

Liang, X., Litkey, P., Hyyppa, J., Kaartinen, H., Vastaranta, M., Holopainen, M., 2012: Automatic Stem Mapping Using Single-Scan Terrestrial Laser Scanning. *IEEE Trans. Geosci. Remote Sens.*, *50*(2), 661–670. doi.org/10.1109/TGRS.2011.2161613.

Lin, Y.-C., Manish, R., Bullock, D., Habib, A, 2021: Comparative Analysis of Different Mobile LiDAR Mapping Systems for Ditch Line Characterization. *Remote Sens.*, *13*(13). doi.org/10.3390/rs13132485.

Luhmann, T., Robson, S., Kyle, S., Boehm, J., 2020: *Close-Range Photogrammetry and 3D Imaging*. De Gruyter. doi.org/doi:10.1515/9783110607253.

Magnusson, M., Lilienthal, A., Duckett, T., 2007: Scan registration for autonomous mining vehicles using 3D-NDT. *J. Field Robot.*, *24*(10), 803–827. doi.org/10.1002/rob.20204.

Méndez, V., Pérez-Romero, A., Sola-Guirado, R., Miranda-Fuentes, A., Manzano-Agugliaro, F., Zapata-Sierra, A., Rodríguez-Lizana, A., 2019: In-Field Estimation of Orange Number and Size by 3D Laser Scanning. *Agronomy*, *9*(12). doi.org/10.3390/agronomy9120885.

Mikhail, E. M., 1976: *Observations and least squares*. University Press of America, Washington, DC.

Monji-Azad, S., Hesser, J., & Löw, N., 2023: A review of non-rigid transformations and learning-based 3D point cloud registration methods. *ISPRS J. of Photogramm. and Remote Sens.*, *196*, 58–72. doi.org/10.1016/j.isprsjprs.2022.12.023.

Riveiro, B., Lindenbergh, R. (Eds.), 2019: *Laser Scanning: An Emerging Technology in Structural Engineering*. CRC Press, Boca Raton. doi.org/10.1201/9781351018869.

Roitsch, T., Cabrera-Bosquet, L., Fournier, A., Ghamkhar, K., Jiménez-Berni, J., Pinto, F., Ober, E. S., 2019: Review: New sensors and data-driven approaches—A path to next generation phenomics. *Plant Sci.*, *282*, 2–10. doi.org/10.1016/j.plantsci.2019.01.011.

Shan, J., Toth, C. K., 2018: *Topographic Laser Ranging and Scanning: Principles and Processing*. 2nd ed., CRC Press, Boca Raton.

Shao, J., Zhang, W., Mellado, N., Wang, N., Jin, S., Cai, S., Luo, L., Lejemble, T., Yan, G., 2020: SLAM-aided forest plot mapping combining terrestrial and mobile laser scanning. *ISPRS J. Photogramm. Remote Sens.*, *163*, 214–230. doi.org/10.1016/j.isprsjprs.2020.03.008.

Vosselman, G., Mass, H.-G., 2010: *Airborne and Terrestrial LASER Scanning*. Whittles Publishing, Dunbeath.

Wolf, P. R., Dewitt, B. A., Wilkinson, B. E., 2014: *Elements of Photogrammetry with Applications in GIS.* 4th ed., McGraw-Hill Education, New York.

Wu, D., Johansen, K., Phinn, S., Robson, A., 2020: Suitability of Airborne and Terrestrial Laser Scanning for Mapping Tree Crop Structural Metrics for Improved Orchard Management. *Remote Sens., 12*, 1647. doi.org/10.3390/rs12101647.

Xu, N., Li, Z., Kang, J., Meng, Q., Niu, M., 2024: Agricultural Vehicle Automatic Navigation Positioning and Obstacle Avoidance Technology Based on ICP. *IEEE Access*, *12*, 85940–85954. doi.org/10.1109/ACCESS.2024.3402743.

Zhang, W., Qi, J., Wan, P., Wang, H., Xie, D., Wang, X., Yan, G., 2016: An Easy-to-Use Airborne LiDAR Data Filtering Method Based on Cloth Simulation. *Remote Sens., 8*(6). doi.org/10.3390/rs8060501.

Zhang, Z., Deriche, R., Faugeras, O., Luong, Q.-T., 1994: A robust technique for matching two uncalibrated images through the recovery of the unknown epipolar geometry. INRIA Rapport de Recherche, 2273, 39 pp.